

A Study on the Change of Barrier Shape for Design of IPMSM Rotor Stress Reduction

Hui-Seong Shin

Master's course, Department of Electrical Engineering, Hanbat National University, Dongseo-Daero, Daejeon, 34158 Korea

In-Soo Song

Master's course, Department of Electrical Engineering, Hanbat National University, Dongseo-Daero, Daejeon, 34158 Korea

Cheol-Min Kim

Bachelor's course, Department of Electrical Engineering, Hanbat National University, Dongseo-Daero, Daejeon, 34158 Korea

Ki-Chan Kim^{*}

Professor, Department of Electrical Engineering, Hanbat National University, Dongseo-Daero, Daejeon, 34158 Korea
kckim@hanbat.ac.kr

Abstract

Most electric vehicles are driven by Interior Permanent Magnet Synchronous Motor (IPMSM) capable of constant power operation in a wide driving range. IPMSM has a structure in which a permanent magnet is embedded in a barrier inside the rotor, and the shape of the barrier has a large effect on the electromagnetic characteristics. The barrier is sensitive to mechanical stiffness as well as electromagnetic properties, and the stress of the rotor is mostly concentrated on the barrier. This paper analyzes electromagnetic properties and mechanical stress through FEM(Finite Element Method) analysis. The stress concentrated in the barrier region was improved while maintaining the electromagnetic properties of the IPMSM used in the study.

Keywords: Electric Vehicle, PMSM, Barrier, Rotor stress reduction, Mechanical stiffness, FEM.

1. Introduction

The IPMSM used in electric vehicles has very different characteristics depending on the shape of the permanent magnet used. The torque of the IPMSM is composed of the sum of the reluctance torque and the magnetic torque. And in the field-weakening control area, the use of the reluctance torque increases compared to the magnetic torque. The reluctance torque is determined by the salient ratio, which is the ratio of the q-axis and d-axis inductance. Therefore, to increase the salient ratio, a barrier structure that increases the q-axis inductance is required. And this structure concentrates the rotor stress on the barrier. To improve structural safety in the high-speed area, the stress concentrated on the barrier

should be relieved. In this study, a barrier design was performed to relieve stress concentrated on the barrier while improving the electromagnetic properties of V-Shape IPMSM through FEM(Finite Element Method) analysis[1-5]. If the barrier shape is designed so that the stress can be improved, the electromagnetic characteristics can be significantly different compared to the existing model because the magnetic path inside the rotor changes. Therefore, it was necessary to first select a model whose electromagnetic characteristics differed within 5% from the existing model. In addition, it was hypothesized that the reduction of the q-axis inductance accompanying the improvement of the rotor stress could be improved by applying a notch at the end of the barrier.

2. Design conditions for FEM analysis

2.1. Base Model Analysis

Figure 1 shows the shape of the 300kW class IPMSM used for FEM analysis. It consists of 8 poles and 72 slots and operates with a torque of 1800Nm at base speed. Since the base speed and the max speed are about 7000rpm different, the use of reluctance torque is important in the field-weakening area. Therefore, the saliency ratio was designed to be large[6,7,8].

In this study, stress concentrated on the rotor barrier was analyzed through FEM. The magnet of the rotor is composed of two layers of V-shape, and the magnet is designed in four segments to reduce eddy current loss. The d-axis magnetic flux path design was conducted to increase the protrusion ratio. [9,10] The rated speed and the maximum speed were 1600rpm and 8500rpm enabling wide field weakening control. After designing the base model, the stress and electromagnetic properties were analyzed. The improved

model design was carried out by analyzing where the stress of the rotor barrier is concentrated[11,12,13].

analysis.

2.2. Stress Improved Model Design Flow Chart

Figure 2 shows the design flow chart. First, the electromagnetic characteristics are analyzed based on the designed base model. After the stress analysis of the base model, the shape of the part where the stress of the rotor is concentrated is improved and designed. The electromagnetic properties of the improved model and the degree of stress improvement are analyzed.

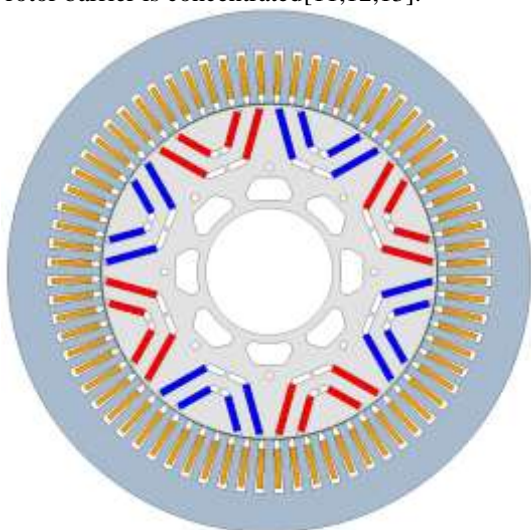


Figure 1. IPMSM base model used for simulation

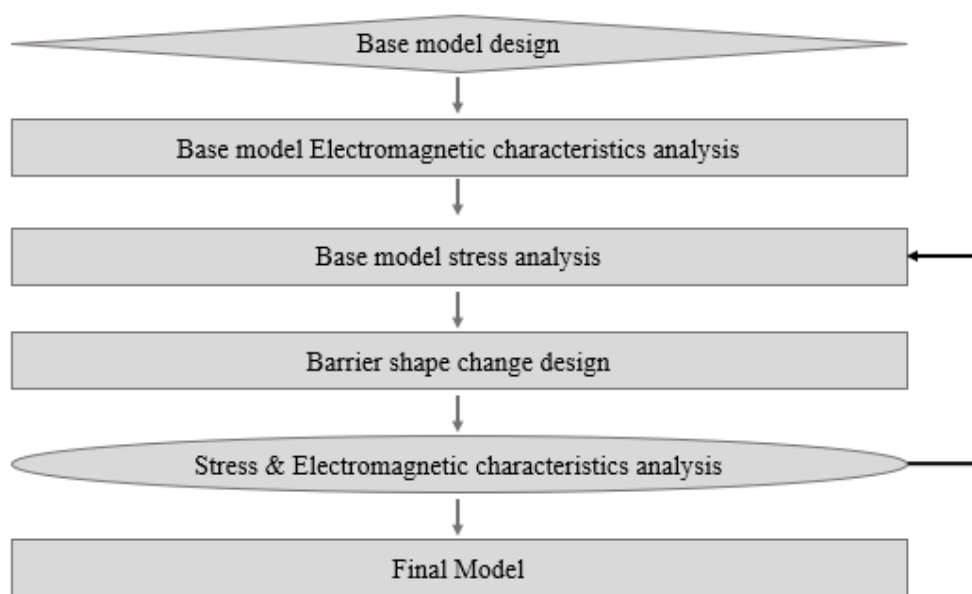


Figure 2. Design flow chart of stress improved model

2.3. Base Model Stress and Electromagnetic Characteristics Analysis

It was impossible to diversify the barrier and notch structures to design the electromagnetic characteristics to be almost identical to the base model. Therefore, after the stress analysis of the base model, the study was conducted in the

direction of designing an improvement in which the stress of the rotor is concentrated[14-17].

Figure 3 shows the barrier shape and stress analysis results of the base model. As a result of the analysis, the stress is concentrated in the part where the barrier of the magnet and the rotor closes.

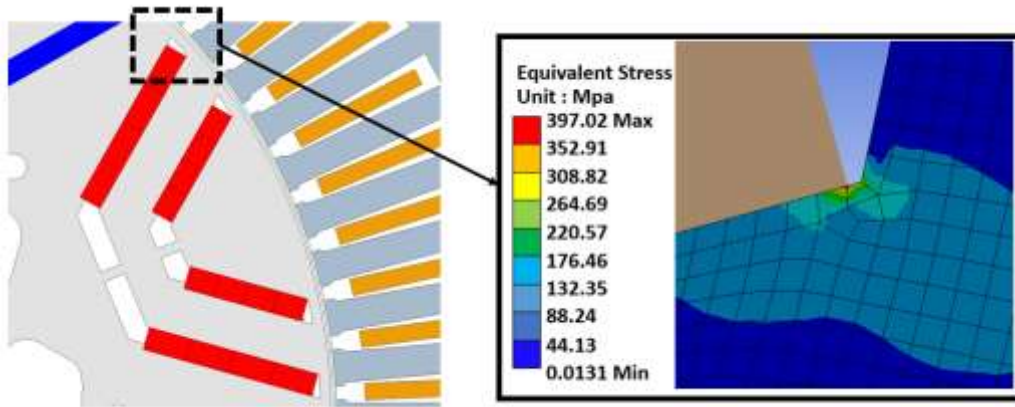


Figure 3. Barrier shape and stress analysis result of the base model

Electromagnetic properties were also analyzed. Based on the electromagnetic characteristics of the base model, the stress improvement design of the rotor was performed. Figure 4 shows the TN and PN curves of the base model.

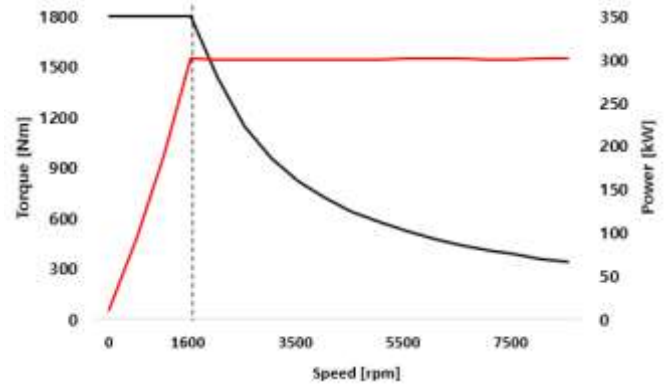


Figure 4. TN curve and PN curve of the base model

2.4. Stress Improved Model Design

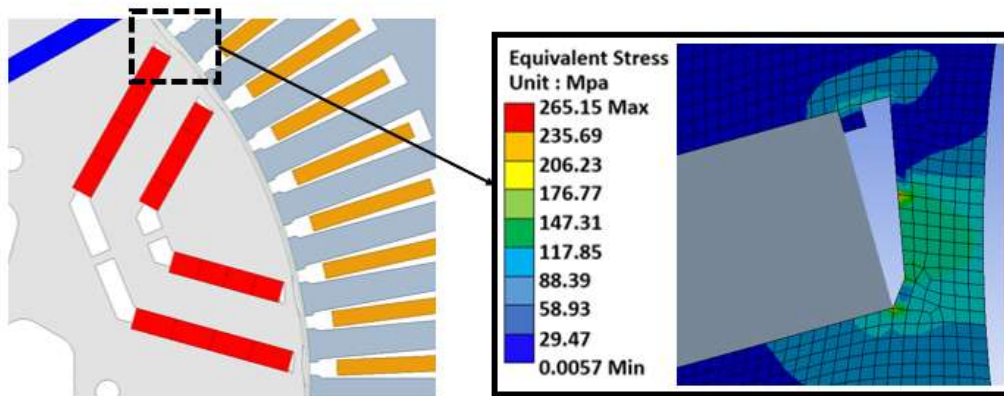


Figure 5. Shape and stress analysis result of stress improved model

Figure 5 shows the barrier shape and stress analysis results of the stress improved model. The stress improved model reduced the barrier length to the rotor outer shell compared to the base model. In addition, the angle where the stress-concentrated magnet and barrier meet was cut, and a nochi was applied to the outer shell of the rotor. As a result of the stress analysis, the magnitude of the maximum stress was reduced by about 130Mpa compared to the base model. In addition, the stress that was concentrated in one place was spread over a wide area, and structurally it was significantly stabilized.

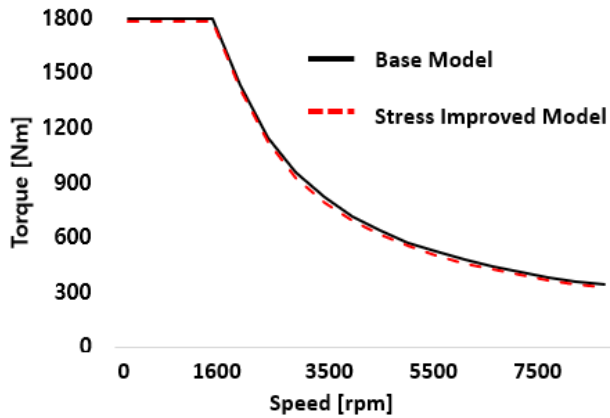


Figure 6. TN curve of base model and stress improved model

Figure 6 shows the TN curve of the base model and stress

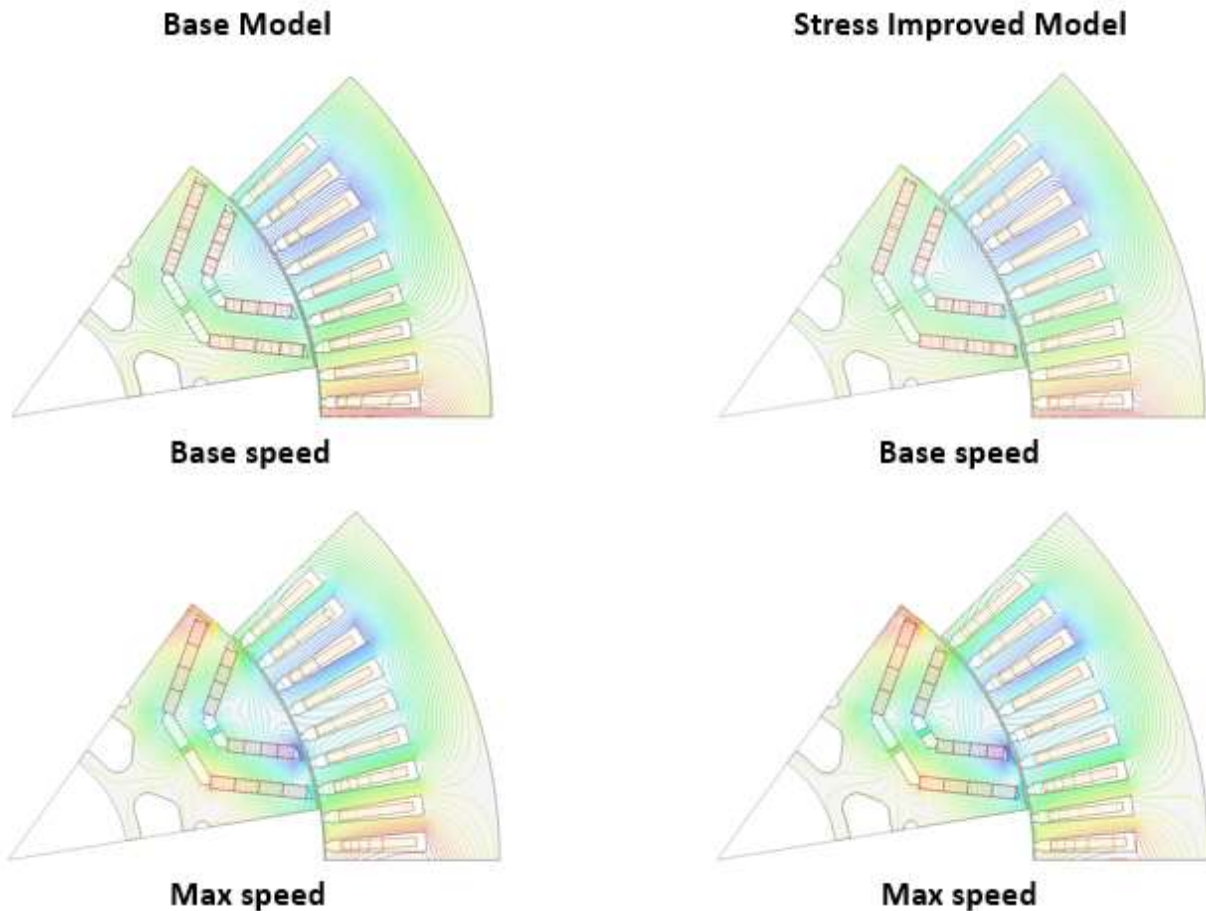


Figure 7. Comparison of magnetic flux lines between base model and stress improved model

Figures 7 and 8 show the comparison of magnetic flux lines

improved model. The TN curve of stress improved model in Figure 6 is the TN curve at the same point as the control point of the base model, and it is the curve when the same current and current phase angle are applied. When the same current was applied at the base speed, the stress improved model yielded a lower torque of about 20Nm. Since the length of the air gap included in the q-axis magnetic path is increased, about 9A more is applied to generate the same torque as the base model at the base speed, and the torque ripple increases by about 0.1%. However, at max speed, the operation depends more on the reluctance torque than on the magnetic torque. Accordingly, the applied current is reduced by about 22A, and the torque ripple is reduced by 1%. Electromagnetic properties showed better properties than the base model, and improved results were obtained in terms of rotor stress.

2.5 Comparison of base model and stress improved model

and magnetic flux density between the base model and the stress improved model.

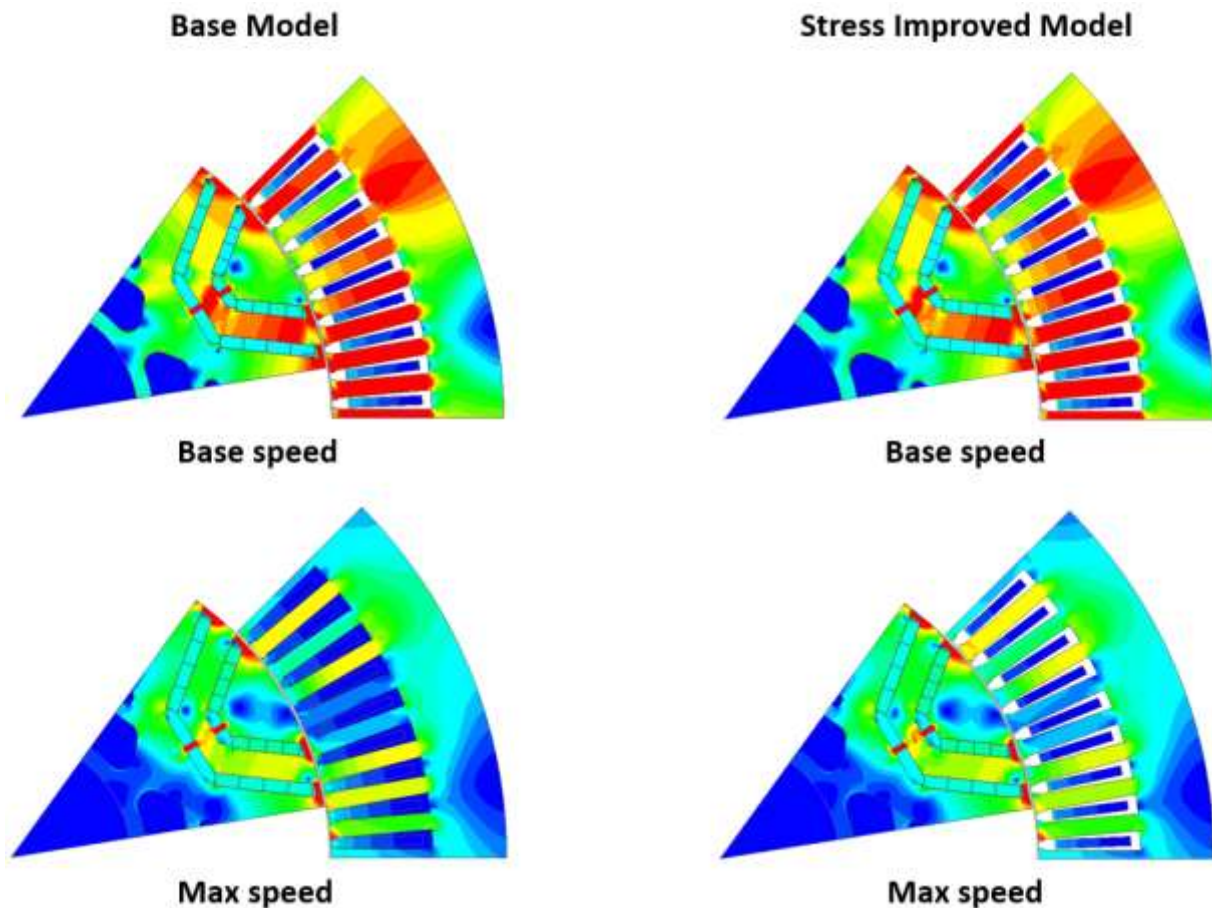


Figure 8. Comparison of magnetic flux density between base model and stress improved model

Although the difference in electromagnetic characteristics is not large, looking at the magnetic flux density distribution in Figure 8, the saturation of the magnetic flux path between the magnet layers of the stress improved model is reduced.

3. Conclusion

As a result of calculating the safety factor through the material data of the steel plate used in the FEM analysis model, the safety factor of the optimal model was improved to about 1.40 compared to the safety factor of about 1.05 of the existing model. Through this study, it can be applied to the design of improving rotor stress and torque ripple for electric vehicles.

4. Acknowledge

This work was supported by the Korea Institute of Energy Technology Evaluation and Planning(KETEP) and the Ministry of Trade, Industry & Energy(MOTIE) of the Republic of Korea (No. 20204030200080).

This work was supported by the Technology Innovation Program (20011435, Development of large capacity Etransaxle and application technology of 240kW class in integrated rear axle for medium and large commercial vehicles) funded By the Ministry of Trade, Industry & Energy(MOTIE, Korea).

5. Reference

1. Spargo, C. M., Mecrow, B. C., & Widmer, J. D, "A seminumerical finite-element postprocessing torque ripple analysis technique for synchronous electric machines utilizing the air-gap Maxwell stress tensor", IEEE transactions on magnetics, 50(5), 1-9, 2013.
2. Kumar, S., Lipo, T. A., & Kwon, B. I, "A 32 000 r/min axial flux permanent magnet machine for energy storage with mechanical stress analysis", IEEE Transactions on Magnetics, 52(7), 1-4, 2016.
3. Zhu, X., Wu, W., Yang, S., Xiang, Z., & Quan, L, "Comparative design and analysis of new type of flux-intensifying interior permanent magnet motors with different q-axis rotor flux barriers", IEEE Transactions on Energy Conversion, 33(4), 2260-2269, 2018.
4. Yamazaki, K., & Aoki, A, "3-D electromagnetic field analysis combined with mechanical stress analysis for interior permanent magnet synchronous motors", IEEE Transactions on Magnetics, 52(3), 1-4, 2015.
5. Jun, C. H., & Nicolas, A "Analysis of the mechanical stresses on a squirrel cage induction motor by the finite element method", IEEE transactions on magnetics, 35(3), 1282-1285, 1999.
6. Ahn, J. H., Choi, J. Y., Park, C. H., Han, C., Kim, C. W., & Yoon, T. G, "Correlation between rotor vibration and mechanical stress in ultra-high-speed permanent magnet synchronous motors", IEEE Transactions on Magnetics, 53(11), 1-6, 2017.

7. Tarek, M. T. B., & Choi, S. (2017, October). Design and rotor shape modification of a multiphase high speed permanent magnet assisted synchronous reluctance motor for stress reduction. In 2017 IEEE energy conversion congress and exposition (ECCE), 5389-5395.
8. Acebal, R., "Effect of shape factor, operating stresses, and electrical conductors on the energy density of rotating machines", IEEE transactions on magnetics, 32(2), 421-425, 1996.
9. Yamazaki, K., Mukaiyama, H., & Daniel, L, Effects of multi-axial mechanical stress on loss characteristics of electrical steel sheets and interior permanent magnet machines. IEEE Transactions on Magnetics, 54(3), 1-4, 2017.
10. DI NARDO, Mauro, et al. "End barrier shape optimizations and sensitivity analysis of synchronous reluctance machines" In: IECON 2015-41st Annual Conference of the IEEE Industrial Electronics Society. IEEE, 002914-002919, 2015.
11. Yamazaki, K., & Kato, Y, "Iron loss analysis of interior permanent magnet synchronous motors by considering mechanical stress and deformation of stators and rotors" IEEE transactions on magnetics, 50(2), 909-912, 2014.
12. Jung, J. W., Lee, B. H., Kim, D. J., Hong, J. P., Kim, J. Y., Jeon, S. M., & Song, D. H, "Mechanical stress reduction of rotor core of interior permanent magnet synchronous motor" IEEE Transactions on Magnetics, 48(2), 911-914, 2012.
13. Yamazaki, K., & Kato, Y, "Optimization of high-speed motors considering centrifugal force and core loss using combination of stress and electromagnetic field analyses" IEEE transactions on magnetics, 49(5), 2181-2184, 2013.
14. Barcaro, M., Meneghetti, G., & Bianchi, N, "Structural analysis of the interior PM rotor considering both static and fatigue loading" IEEE Transactions on Industry Applications, 50(1), 253-260, 2013.
15. Kolehmainen, J, "Synchronous reluctance motor with form blocked rotor" IEEE Transactions on Energy Conversion, 25(2), 450-456, 2010
16. CREDO, Andrea, et al. Synchronous reluctance motors with asymmetric rotor shapes and epoxy resin for electric vehicles. In: 2019 IEEE Energy Conversion Congress and Exposition (ECCE). IEEE, 4463-4469, 2019.
17. Hyun-Seob Cho. "Design of Noise Reduction Output Filter for Induction Motor Using H-Bridge Inverter" Journal of Next-generation Convergence Technology Association, 4(6):595-600, 2020 December.